A novel treatment strategy for preterm birth: Intra-vaginal progesterone-loaded fibrous patches

Muhammet Emin Cam[a,b,c,*], Ayse Nur Hazar-Yavuz[c], Sumeyye Cesur[b,d], Ozan Ozkan[e], Hilal Turkoglu Sasmazel[e], Mehmet Sayip Eroglu[f,g], Francis Brako[a,h], Jubair Ahmed[a], Levent Kabasakal[c], Guogang Ren[i], Oguzhan Gunduz[b,d], Mohan Edirisinghe[a,*]

[a]Department of Mechanical Engineering, University College London, Torrington Place, London WC1E 7JE, UK

[b]Center for Nanotechnology and Biomaterials Application and Research, Marmara University, Istanbul 34722, Turkey

[c]Department of Pharmacology, Faculty of Pharmacy, Marmara University, Istanbul 34668, Turkey

[d]Department of Metallurgy and Material Engineering, Faculty of Technology, Marmara University, Istanbul 34722, Turkey

[e]Department of Metallurgical and Materials Engineering, Faculty of Engineering, Atilim University, 06836 Ankara, Turkey

[f]Department of Chemical Engineering, Marmara University, Faculty of Engineering, Goztepe Campus, 34722 Kadikoy/Istanbul, Turkey

[g]TUBITAK-UME, Chemistry Group Laboratories, 41470 Gebze/Kocaeli, Turkey

[h]School of Pharmacy, University College London, 29-39 Brunswick Square, London WC1N 1AX, UK

[i]Mechanical and Mechatronics Engineering Division, School of Engineering and Technology, University of Hertfordshire, UK

*Corresponding authors:

e-mail: m.cam@ucl.ac.uk and m.edirisinghe@ucl.ac.uk

ABSTRACT

Progesterone-loaded poly(lactic) acid fibrous polymeric patches were created for the intra-vaginal application using electrospinning (ES) and pressurized gyration (PG) to prevent preterm birth with higher bioavailability. The patches were intravaginally inserted into the rats in the final week of their pregnancy, equivalent to the third trimester of human pregnancy. Maintenance tocolysis with progesterone-loaded patches was elucidated by recording the contractile response of uterine smooth muscle to noradrenaline in pregnant rats. Both progesterone-loaded patches indicated similar results from the release and thermal studies, however, patches obtained by ES had smaller average diameters and more uniform dispersion compared to PG. Patches obtained by PG had better results in production yield and tensile strength than ES; thereby PG is better suited for scaled-up production. The patches did not affect the cell attachment, viability and proliferation on Vero cells negatively. Consequently, progesterone-loaded patches are a novel and successful treatment strategy for preventing preterm birth.

Keywords: Progesterone; pressurized gyration; electrospinning; fibrous polymeric patch; preterm birth; organ bath

1. Introduction

Preterm birth, also commonly referred to as premature birth, is the birth of a baby which has completed less than 37 weeks of gestation, it is a leading cause of infant mortality under the age of five and it is one of the most crucial research areas in need of new treatment strategies (Kindinger et al., 2017). Around 15 million babies suffer from preterm birth and the number is increasing. Annual health costs associated with surviving babies in the US exceed $ 25 billion per year and climbing (McCormick et al., 2011).

Preterm birth is a syndrome attributed to heterogeneous influences such as a downfall in the action of progesterone (P4), infection, multiple gestations, and cervical disease (Goldenberg et al., 2008). P4, which is a steroid hormone, is a primary prescribed treatment for pre-term births and plays a crucial role in female reproduction with regulatory actions throughout the female reproductive axis but the mechanism of action is not clear (Graham and Clarke, 1997). P4 may work by activating the anti-inflammatory and pro-relaxation pathways in the uterus, thereby reducing uterine contractility and preventing the onset of premature birth. The rate of preterm birth had declined widely due to P4 treatment in women who are at high risk for preterm birth due to a history of preterm birth or a short cervical length (Nold et al., 2013).

P4 is a poorly water-soluble drug (Cam et al., 2019b) traditionally available in tablet and also gelatinized capsule, vaginal gel, vaginal insert, and injection forms. All forms are daily given except the injection form, which is weekly given. P4 administered orally can cause sleepiness, headaches, back pain, abdominal cramps, constipation, breast tenderness, nausea, dizziness, edema, hypotension, dysphoria, fatigue and may induce

a hypercoagulant state. Taking into account all of these, one of the greatest advantages of P4 given via the vaginal route is its high bioavailability in the uterus as the first pass through the liver is avoided. Although vaginal irritation can be uncomfortable, this route allows for fewer systemic side effects (Goletiani et al., 2007).

Fibrous patches are recognized to be the most prominent micro/nanostructured materials that are presently used in various applications such as bioengineering, healthcare and environmental applications. In addition, fibrous patches have very significant advantages such as high permeability, high surface area to volume ratio, low basis weight, high density of pores and low fiber diameter (Balamurugan et al., 2011). The fibrous patches produced with natural and synthetic polymers have been found to be promising for developing drug delivery systems in several methods. One of the most common and preferred techniques to produce fibrous patches is via electrospinning (ES) (Huang et al., 2020; Qin et al., 2019). Moreover, a variety of techniques have been available recently to produce fibrous patches for biomedical applications, one such method is pressurized gyration (Alenezi et al., 2019). Previously, patches for hormone delivery, with some advantages such as controlled release and efficient drug loading, have been produced by ES and PG (Brako et al., 2018; Mofidfar and Prausnitz, 2019).

ES is an effective method for making continuous polymeric micro/nanofibrous patches (Figuer 1). The ES method of producing fibrous patches is attractive owing primarily to its cost-effectiveness, reproducibility, simplicity and ability to spin a wide range of polymers whilst ensuring the opportunity for direct encapsulation of medicines into the electrospun fibrous patches. Several variable parameters such as polymer

92 solution feed rate, solution composition and applied voltage affect the characteristics of
93 the electrospun fibrous patches (Cam et al., 2019a; Cam et al., 2020).

94 An original pressure driven technique for the production of fibrous patches has been
95 established to incorporate concurrent use of pressure, flow, and rotation. The solvent-
96 based production technique, pressurized gyration (PG), simultaneously exploits
97 centrifugal spinning and solution blow spinning to produce fibrous patches (Figure 1).
98 PG offers an alternative option to electric-field driven technologies such as ES. The
99 advantages of PG include the ability to spin charge-absent polymers and a high
100 production yield. PG has a much larger production capacity compared to other
101 generation methods such as ES (Raimi-Abraham et al., 2015). The PG system consists
102 of a rotating perforated chamber, which is fed with a polymer solution, containing a
103 series of orifices (24) with dimensions of 0.5 mm on its midline circumference. The
104 rotating speed (12000-36000 rpm) of the chamber and the pressurized gas ($1x10^5$-
105 $3x10^5$ Pa) affects the characteristics of fibers in terms of final morphology. Essentially,
106 the polymer solution in the chamber is extruded out from the orifices following the
107 rotation of the chamber, and dry fibrous patches are obtained following solvent
108 evaporation of the extruded polymer solution (Heseltine et al., 2018).

109 In our study, we aim to produce a patch that can be administered vaginally, thus
110 reducing side effects, as well as providing a higher bioavailability and reducing the
111 frequency of dosage. Moreover, the larger production capacity of PG for the production
112 of P4-loaded fibrous patches was evaluated and compared to ES. P4-loaded fibrous
113 patches were produced with two different techniques: ES and PG. These fibrous
114 patches are compared with respect to their ability to increase the dissolution of the

poorly soluble drug P4 and also the drug incorporation, characterization, release characteristics, tensile strength, short-term cell attachment, long-term viability, and cell proliferation have been tested. In addition, the effect of maintenance tocolysis with P4-loaded fibrous polymeric patches were examined in the uterus of pregnant rats using organ bath experiment, and also compared with oral route (Figure 1).

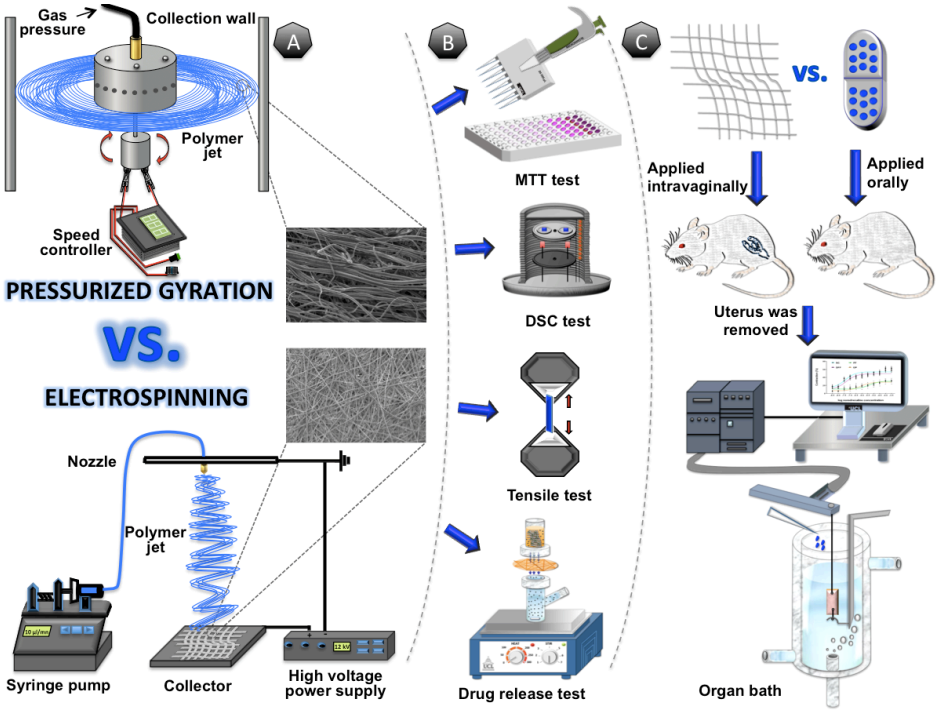

Figure 1. Schematic illustration of the experiments. (A) production processes of progesterone-loaded fibrous patches of two different techniques; electrospinning and pressurized gyration, (B) characterization of produced fibrous patches, (C) comparisons of the tocolytic effects of progesterone-loaded fibrous patch and oral progesterone using organ bath experiments.

2. Materials and methods

2.1 Materials

Poly(lactic acid) (PLA) was obtained from Nature Works LLC, Minnetonka, MN. Progesterone (P4, Mw ~ 314 g mol^{-1}, aqueous solubility: 8.81 mg/L (at 25°C), log P: 3.87), (-)-noradrenaline (Mw ~ 169.18 g mol^{-1}), chloroform (99.9%, v/v), phosphate buffer saline (PBS), Dulbecco's Modified Eagle Medium (DMEM/F12), penicillin/streptomycin, fetal bovine serum (FBS), 3-(4,5-dimethyl-2-thiazolyl)-2,5-diphenyl-2H-tetrazolium bromide (MTT), dimethylsulfoxide (DMSO), ethanol (99.9%, v/v), paraformaldehyde, Triton X-100, and L-glutamine were from Sigma-Aldrich (UK). Phosphate buffer saline (PBS) and bovine serum albumin (BSA) were obtained from Amresco (USA). Alexa Fluor 488 Phalloidin (AF488) and (4',6-diamidino-2-phenylindole, dihydrochloride) (DAPI) was purchased from Life Technologies (USA). Simulated vaginal fluid (pH = 4.7) was prepared according to the formula developed by Owen and Katz.(Owen and Katz, 1999) All chemical and biological agents were cell culture grade and used as received without further sterilization.

2.2 Preparation and Characterization of Solutions

The polymer solutions were prepared with the mixtures of PLA, P4 and chloroform as a solvent, by continuous magnetic stirring. Firstly, PLA was dissolved in chloroform at four different concentrations of 8, 10, 12 and 15% (w/v) and then P4 (10%, w/w) was added to solution at the ambient temperature (25°C) and mixed for almost an hour. The physical parameters such as viscosity, surface tension, electrical conductivity and density for the solutions were measured by viscometer (Brookfield DV-111, Harlow,

UK), force tensiometer (Kruss K9, Hamburg, Germany), electrical conductivity probe (Cond 3110 SET 1, WTW, Germany) and density bottle (10 mL specific density bottle, Boru Cam Inc., Turkey). All the measurements were repeated three times at ambient temperature. These equipments were calibrated prior to measurements.

2.3 Fibrous Patch Preparation and Characterization

Pure and P4-loaded PLA fibrous patches were produced in four different polymer concentrations (8, 10, 12 and 15%, w/v) with a constant P4 ratio (10%, w/w) by PG at ambient temperature (25°C) and humidity (56%) using a method described previously (Mahalingam and Edirisinghe, 2013). According to the results obtained from scanning electron microscopy (SEM) of fibrous patches produced by PG, optimal ratio was chosen and this ratio was used for ES. In brief, 10 ml of drug-polymer mixture was prepared using chloroform and placed in an aluminum vessel and spun at a rotational speed of 12000-36000 rpm and a working pressure of 0.1 MPa to produce P4-loaded fibrous patches (Table S1A, Supplementary Data).

The morphology and size of the fibrous patches were investigated using SEM. Post-decision on the optimal polymer ratio of the fibrous patches produced by pressurized gyration, fibrous patches were produced using ES at 12% (w/v) PLA and 10% (w/w) P4. For the ES procedure, two working distances (13 and 15 cm), three flow rates (10, 20 and 30 µl/min) and four voltages (6, 8, 10, 12 kV) were used (Table S1B, Supplementary Data). The material compositions were investigated using thermal and spectroscopic techniques.

2.4 Scanning Electron Microscopy

The morphologies of the composite fibrous patches were investigated with scanning electron microscopy (JCM-5700, JEOL, Japan). The surface of the samples was gold sputter coated for 60 seconds. The average fiber diameter and their distribution were determined by using the software ImageJ (Brocken Symmetry Software).

2.5 Attenuated Total Reflection-Fourier Transform Infrared Spectroscopy (ATR-FTIR).

ATR–FTIR measurements were performed using Bruker Vertex 90 spectrometer and spectrographs were examined using OPUS Viewer version 6.5 software for analyzing molecular contents of fibrous patches and to confirm the presence of P4 into the fibrous patches.

2.6 X-ray Powder Diffraction

D/Max-BR diffractometer (RigaKu, Tokyo, Japan) with Cu Kα radiation was used to analyze structure and crystalline forms of the fibrous patch contents. Analyses were performed at 40 mV and 30 mA over 2θ range of 5–60° at a rate of 2°/min. OriginPro 7.0 software (OriginLab Corporation, MA, USA) was used to convert the obtained data to diffractograms and for their evaluation.

2.7 Differential Scanning Calorimetry (DSC)

Differential scanning calorimetry (DSC) measurements were conducted using Perkin Elmer Jade DSC and Pyris software (PerkinElmer Inc., Mass., USA) at a heating rate of 10°C min^{-1} between 0 and 300°C under dynamic argon atmosphere (20 ml min^{-1}) to determine thermal properties of the fibrous patches. Temperature

calibration of DSC was performed according to the indium melting point and melting enthalpy.

2.8 Drug Encapsulation Efficiency

A standard assay procedure was used to determine the P4 content inside the fibrous patches. The fibrous patches dissolved completely in chloroform and were detected by UV at 270 nm (Wilson, 2009). P4-loaded fibrous patch samples were weighed (1 mg) and dissolved into 10 ml of absolute chloroform in a volumetric flask. The flask was stirred gently over a period of 1 h to provide a complete dissolution of P4 into the chloroform. 3 ml of solution was taken and evaluated using a UV-visible spectrophotometer using a wavelength 270 nm (Jenway 6305, Bibby Scientific, Staffordshire, UK). The % encapsulation efficiency was calculated using a calibration equation.

Encapsulation efficiency (%) =

mass of actual drug loaded in fibrous scaffolds/

mass of drug used in fibrous scaffolds fabrication x 100% (1)

2.9 Release Studies

Franz diffusion cells with cellulose acetate membranes of pore size 0.2 μm were used for performing in vitro drug release studies. This approach was chosen for the release study because there would be a close similarity between drug permeation through 0.2 μm acetate membrane and the mucosal membrane (Khdair et al., 2013). 3 ml of PBS, pH 7.4 and a stir bar was placed in the receptor chamber to provide sufficient mixing of P4 transported through the membrane into the PBS in the receptor

chamber of apparatus. The cellulose acetate membrane, which was priorly submerged into simulated vaginal fluid (SVF) for 30 min, was placed onto the receptor chamber. Finally, the donor chamber was mounted onto the receptor chamber and thus the membrane was compressed between two chambers. 1 ml of SVF was put in the donor chamber and fibrous patches containing 10 mg of P4 was placed inside. The Franz diffusion cell was kept at a constant temperature of 37°C. The quantity of drug released through the membrane was measured taking 1 ml aliquots from the receptor chamber at certain times (0.5, 1, 2, 3, 4, 16, 24 h) and quantified using UV spectroscopy.

2.10 Tensile Tests of Fibrous Patches

The tensile strength of fibrous patches was determined and evaluated using an Instron 4411 tensile test machine at ambient conditions (23°C). The results were analyzed using Bluehill 2 software (Elancourt, France). Six fibrous patch (1x5 cm) specimens were tested for each set of samples and the thicknesses of the specimens were measured using a digital micrometer (Mitutoyo MTI Corp., USA). Both ends of each specimen were compressed by the top and bottom grip. They were subjected to a tensile test under conditions of 5 mm min^{-1} test speed and 1 cm distance between grips.

2.11 *In Vitro* Cytotoxicity Studies

In vitro cytotoxicity of the fibrous patches was investigated with a commercial Vero epithelial cell line (ATCC CCL-81) for 7 days according to the literature data (Karuppannan et al., 2017). Samples for the studies were prepared in circular shape with 1 cm diameter cut from the fibrous patches. The samples for both pure and P4-loaded fibrous patches were sterilized with UV (both sides) for 15 min in 24 well plates

prior to the culture and seeded with initial cell concentration of $5x10^4$ cells/ml under standard aseptic conditions. The well plates used were coated with parafilm to prevent cells from attaching/proliferating to the well bottom instead of the test samples. Blank commercial tissue culture polystyrene (TCPS) Petri dishes were used as the control group and seeded with the initial cell concentration as the patch samples. DMEM/F12 supplemented with 10% (v/v) FBS, 1% (v/v) L-glutamine and 1% (v/v) penicillin/streptomycin (100 units/ml penicillin, 100 µg/ml streptomycin) was used as culture medium and refreshed every 24 hours. The cultured samples were incubated under 5% CO_2 at 37°C. The cytotoxicity of the fibrous patches were investigated in terms of initial cell attachment, 7-day viability as well as yield and visual morphology by using haemocytometric counting, MTT colorimetric assay and fluorescence imaging. The control groups were utilized only for attachment, viability and yield studies.

2.11.1 Cell Attachment

The initial cell attachment capability of the fibrous patches was determined for the first 3 h after the initial seeding at 30 min intervals by using haemocytometric cell counting. Briefly, the cultured test samples corresponding to each interval were gently removed from the culture dishes without disturbing the cells attached. The cells in the medium remaining inside the dish wells were then counted. The difference between the initial number of cells seeded and the remaining cells counted in the dish was taken as the number of cells attached to the test sample at that specific time interval. For the control TCPS wells, the cells were counted directly from the medium inside, since there were no test samples to remove. The results were presented as the percent cells attached against time. Then, the ratio of the number of cells attached to the test

sample/TCPS well to the number of cells seeded initially was given as a percentage value to represent the attachment concentration of the test samples/TCPS wells at specific intervals.

2.11.2 Viability and Yield

The viability of the cells seeded was monitored for the total course of the culture conducted for 7 days. MTT colorimetric assay was utilized for every 48 h, starting at the end of the first 24 h of the culture. Briefly, the cultured test samples corresponding to each interval were transferred to a clean Petri dish and gently washed 3 times with PBS. Then the samples were incubated for 3 h with fresh medium containing 10% (v/v) MTT solution. After the incubation, the medium/MTT solution was replaced with DMSO (1 ml/sample) and the samples were incubated for an additional hour. Finally, aliquots of the incubated DMSO solution were transferred into 96 well plates and the cell viabilities of that specific interval for all the test samples were measured in terms of absorbance using a microplate reader at 540 nm. The same protocol was directly applied to the control TCPS wells without transferring the cells to another clean dish. The cell yields at the end of the culture were also calculated from the absorbance values obtained at the 7^{th} day for the test samples as well as the control wells by plotting a calibration curve throughout the culture period. It defines the correlation between the number of viable cells and the corresponding absorbance value.

2.11.3 Visual Inspection

In addition to attachment, viability and yield assays, the cytotoxicity of the test samples obtained from pure and P4-loaded fibrous patches was also investigated visually in order to see if there was any negative effect on the morphology of the cells

cultured. Fluorescence imaging was conducted on the cultured test samples on the 3rd and 7th day with AF-488/DAPI dual staining. Briefly, test samples were transferred to a clean Petri dish on the corresponding days, gently washed with PBS three times and fixed with 4% (v/v) paraformaldehyde for 45 min at ambient temperature (22°C). The fixative was then washed away with PBS again at least 3 times, and the test samples were permeabilized with 0.1% Triton X-100 for 5 min, blocked with BSA for 30 min and finally stained with AF-488 for 20 min and with DAPI for 10 min at the ambient temperature in the dark. Finally, the staining solutions were washed away with PBS twice and the imaging was conducted immediately after using a fluorescent microscope (AMG EVOS-FL, USA) at x10 and/or x40 magnifications. The excitation and the emission wavelengths of AF-488 and DAPI were λ_{ex}: 495 nm and λ_{em}: 518 nm, and λ_{ex}: 345 nm and λ_{em}: 455 nm, respectively.

2.12 In Vivo Testing

All *in vivo* experiments were carried out with the approval of the Marmara University, Animal Experiments Local Ethics Committee (MUHDEK) (permission number: 92.2018.mar). Pregnant Sprague-Dawley rats were obtained from The Experimental Animal Implementation and Research Centre (DEHAMER). The rats were housed under controlled temperature (20-23°C), in humidity (40-60 %) and light (12 h light/dark regime)-regulated rooms. The animals were kept on a standard rodent pellet diet, with tap water available ad libitum.

2.12.1 Experimental Design of *In Vivo* Studies

Pregnant rats were randomly divided into 4 groups of 6 animals as follows: naive control group (NC), drug-free (pure PLA) fibrous patches implantation group (DFF), P4-

loaded fibrous patch/ES implantation group (PF) and oral P4 treatment group (OP). The NC group did not undergo any treatment or implantation during their pregnancy. DFF and PF were implanted with drug-free and P4-loaded fibrous patches respectively on the 15^{th} day of the pregnancy. Oral P4 treatment began on the 15^{th} day of the pregnancy and continued to the 21^{st} day. On the 22^{nd} day of pregnancy, all the rats were decapitated and the uterine tissues were removed.

2.12.2 Implantation of Fibrous Patches Into The Rats

Drug-free fibrous patches and P4-loaded fibrous patches were prepared by cutting an area 10 cm^2 (1 mg P4 in 10 cm^2). Following anesthetization with ether, the fibrous patches pieces were implanted intravaginally to the rats (Kim et al., 2013).

2.12.3. Oral Progesterone In Vivo Treatment

The treatment of the oral P4 group also started on the 15^{th} day of pregnancy. The given P4 was dissolved in olive oil (Hajagos-Tóth et al., 2016) and the administration was given via oral gavage every day up to day 21 in a dose of 50 mg/kg (Khan and Ahmed, 1969).

2.12.4. In Vitro Organ Bath Experiments

2.12.4.1. Uterus Preparation

Uterus were removed from the all 22-day-pregnant rats (250-350 g) (n=6 in each group). 5 mm-long muscle rings were sliced from uterine horns; subsequently, the surrounding mesentery and fat tissues were carefully removed from the uterine rings and rings were mounted vertically in an organ bath containing 20 ml Krebs-Henseleit buffer (KHB; composition: 118 mM NaCl, 4.7 mM KCl, 2.5 mM $CaCl_2$, 1 mM $MgSo_4$, 1

331 mM KH_2PO_4, 25 mM $NaHCO_3$, and 11 mM glucose) at pH 7.40. The temperature of the
332 organ bath was maintained at 37°C, and carbogen (95% O_2 and 5% CO_2 gas mixture)
333 was perfused through the bath. After mounting, the rings were equilibrated for
334 approximately 60 minutes before experiments began; with a buffer change every 15
335 minutes. The initial tension of the preparation was set to about 1 g. The tension of the
336 myometrial rings was measured with a gauge transducer (TDA-94 Commat, Commat
337 LTD., Ankara, Turkey) and recorded on-line on a computer via a four channel
338 transducer data acquisition system using appropriate software (Polywin 95 ver 1.0.
339 Commat, Commat LTD, Ankara, Turkey)

340 **2.12.4.2. Contractility Studies**

341 In the isolated uterine rings, rhythmic contractions were elicited with 124 mM KCl,
342 and cumulative dose-response curves were constructed in each experiment in the
343 presence of (-)-noradrenaline (NA) ($10^{-8.5}$ to $10^{-3.5}$) (Kim et al., 2004). Following the
344 addition of each concentration of (-)-noradrenaline, recordings were taken for 120 s.
345 Concentration-response curves were fitted and areas under the curves (AUC) were
346 evaluated and analyzed statistically with the Prism 6.5 (Graphpad Software Inc. San
347 Diego, CA, USA) computer program. From the AUC values, the maximal inhibitory
348 effect of NA (Emax) and the concentration of NA eliciting 50% of the maximal inhibition
349 of uterine contraction (EC_{50}) values were calculated.

350 **2.13. Statistical Analysis**

351 Values in the animal test were presented as mean ± standard error of the mean,
352 whereas in SEM micrographs, tests were presented as mean ± standard deviation.
353 Differences in the contractile effect of KCl and cumulative NA were analyzed using

354 analysis of variance (ANOVA) tests with the Tukey multiple comparison test.
355 Concentration-response curves were fitted, areas under the curves (AUC) were
356 determined, and Emax and EC_{50} calculated with the Prism 6.5 software. The assays
357 conducted for attachment, viability as well as yield were repeated three times (n = 3) for
358 each type of samples as well as blank controls. The statistical differences were
359 determined with ANOVA followed by Tukey multiple comparison test using IBM SPSS
360 v24.0 Statistics software. Probability of the data was considered statistically significant
361 for p-values less than 0.05 and statistically highly significant for p-values less than 0.01.
362 The results were marked with (*) for $p < 0.05$, (**) for $p < 0.01$.

363

364 # 3. Results

365 ## 3.1. Morphological Characterization of Microfiber

366 The change in the fiber size and morphology of pure and P4-loaded fibrous patches
367 using PG and ES in different polymer concentrations and processing conditions were
368 analyzed using SEM, results are shown in Figure 2. Firstly, fibrous patches of four
369 different PLA concentrations (8%, 10%, 12%, 15%) were produced with and without
370 10% P4 by PG (Figure 2). According to the results obtained from PG, we concluded that
371 adding P4 to the 8% PLA solution created beaded and nonhomogeneous fibers. The
372 diameter of the pure 8% PLA fibrous patches is 7.34 ± 1.11 μm and increased to 7.61 ±
373 1.13 μm by adding P4. With the pure 10% PLA fibrous patches, the diameter of the
374 fibers was 7.92 ± 1.27 μm, it increased slightly to 7.96 ± 1.79 μm by the addition of P4.
375 It is clearly seen that the addition of P4 to 10% PLA solution caused heavily beaded

fibers and loss in homogeneity. The highest production yield per ml solution also belonged to the 12% PLA solutions obtaining 102.4 mg/ml in pure fibrous patches and 114.7 mg/ml in P4-loaded fibrous patches compared to other concentrations. The production yields per ml solution with the same polymer ratio by ES were 78.2 mg/ml in pure fibrous patches and 86.7 mg/ml in P4-loaded fibrous patches. The diameter of pure 12% PLA (6.76 ± 1.82 μm) fibrous patches increased by adding P4 (12.36 ± 3.60 μm). The diameters of pure 15% PLA fibrous patches (26.29 ± 4.69 μm) and also with P4 (24.25 ± 2.40 μm) were much greater and were not investigated further. In summary, 12% PLA was chosen for the further tests and forming of fibrous patches using both PG and ES, the latter was with different process conditions directly related to ES (Table S1, Supplementary Data).

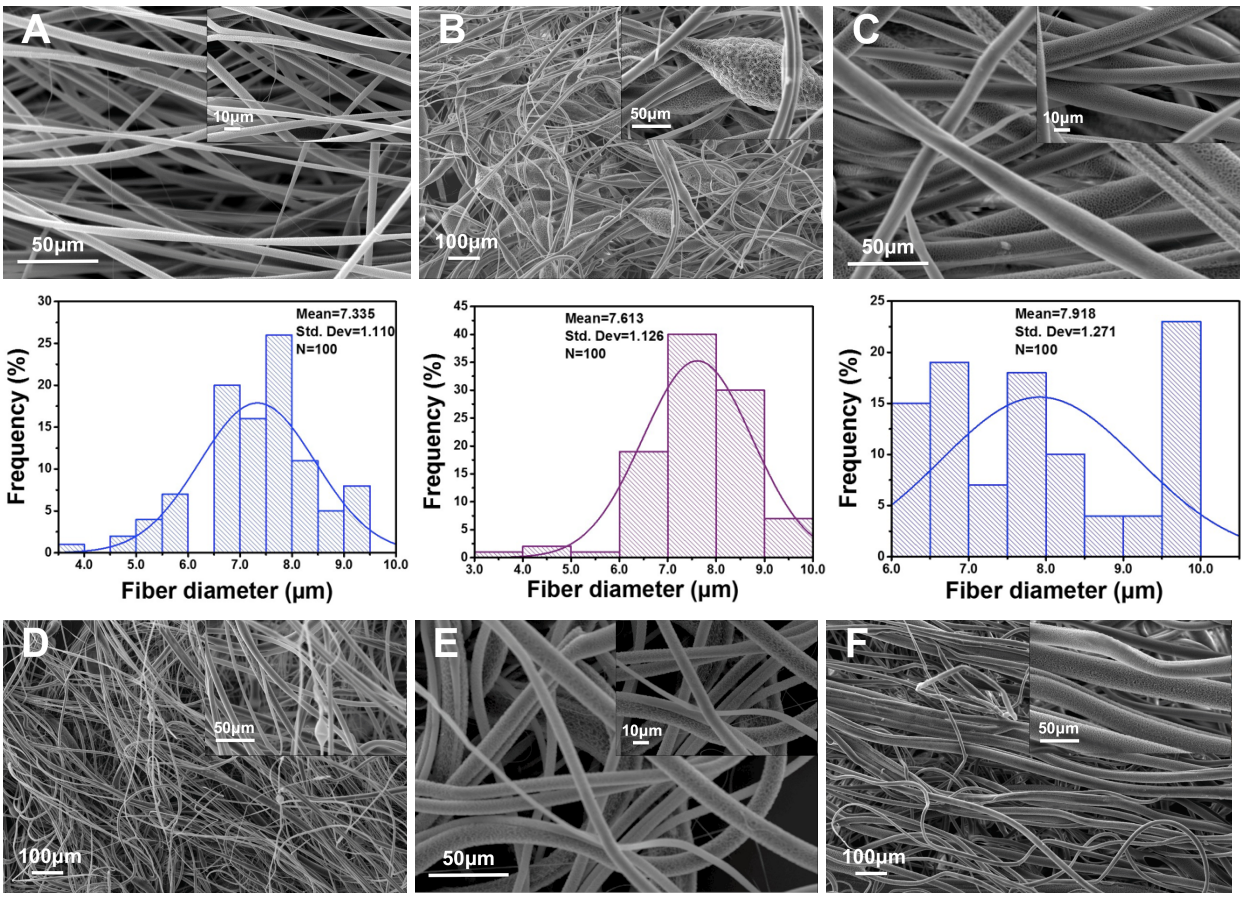

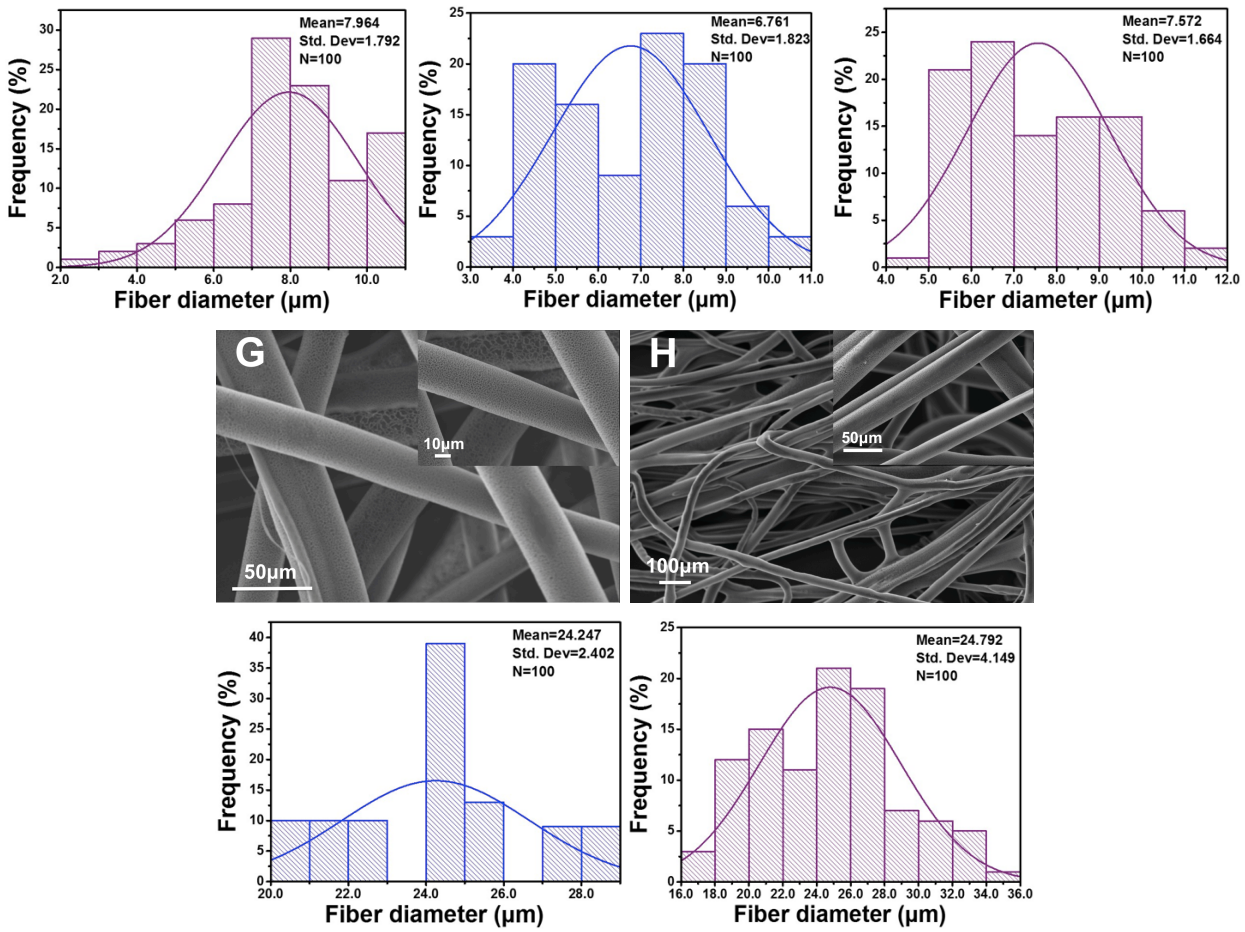

Figure 2. SEM images and fiber diameter distributions of pure and P4-loaded fibrous patches produced by PG. (A) 8% (w/v) PLA, (B) P4-loaded 8% PLA, (C) 10% PLA, (D) P4-loaded 10% PLA, (E) 12% PLA, (F) P4-loaded 12% PLA, (G) 15% PLA, and (H) P4-loaded 15%. In all diameter distributions, n = 100.

In the production of pure fibrous patches using ES, when the flow rate and applied voltage remained constant and working distance increased, the diameter of fibrous patches decreased (Figure 3A to 3F). In comparison, at 20 μl/min flow rate and 8 kV applied voltage, working distance was changed from 15 cm to 13 cm and the diameter of fibrous patches increased from 6.86 ± 1.30 μm to 7.11 ± 1.29 μm. In another sample, at 30 μl/min and 10 kV, the diameter of fibrous patches increased from 6.41 ± 1.40 μm

to 7.02 ± 1.39 µm when the working distance was changed from 15 cm to 13 cm. Optimized fibrous patches were produced at 13cm, 10 µl/min, 6 kV process conditions due to smaller diameters (6.09 ± 0.96 µm) and higher uniformity.

In the forming of P4-loaded fibrous patches using ES, when the working distance and applied voltage remained constant and flow rate increased, the diameter of fibrous patches increased (Figure 3G to 3L). Thus at 15cm and 12 kV, increasing the flow from 10 to 30 µl/min caused the diameter of fibrous patches to increase from 7.22 ± 1.09 to 7.89 ± 1.38 µm. The same effect was observed in other samples. Thus, fibrous patch forming by ES was optimized at in 15cm, 10 µl/min, and 12 kV process conditions due to thinner diameter (7.22 ± 1.09 µm) and higher homogeneity. We used the optimized sample in our further studies described below. The details of the physical properties of solutions are illustrated in Electronic Supplementary Data, moreover, ES and PG process conditions were given in details in Electronic Supplementary Data.

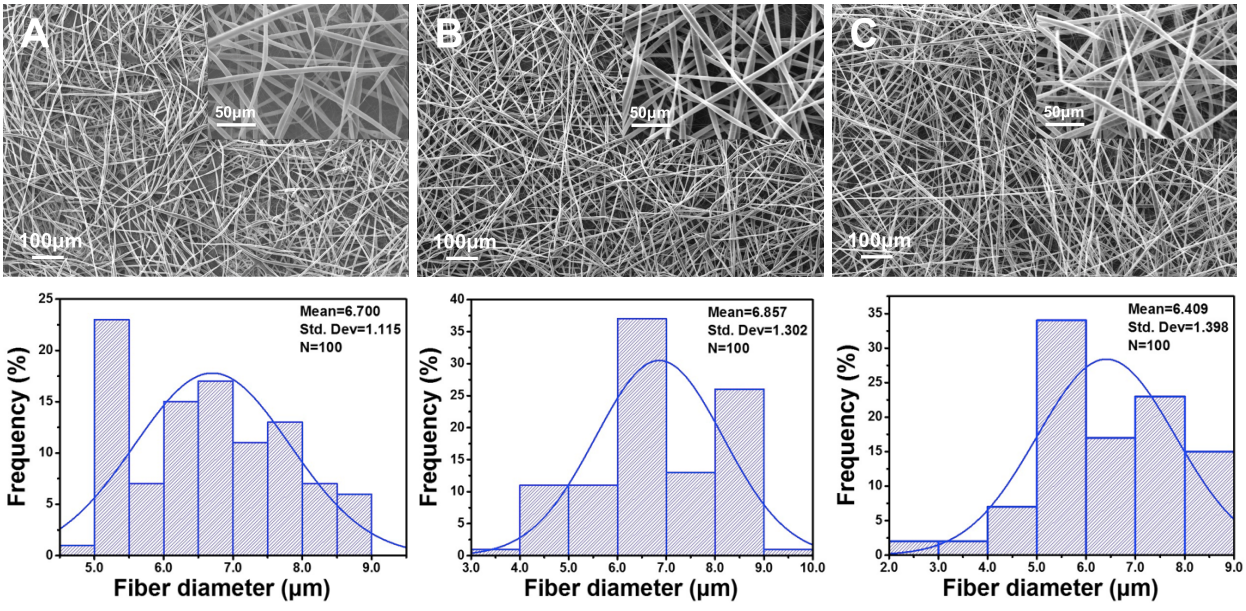

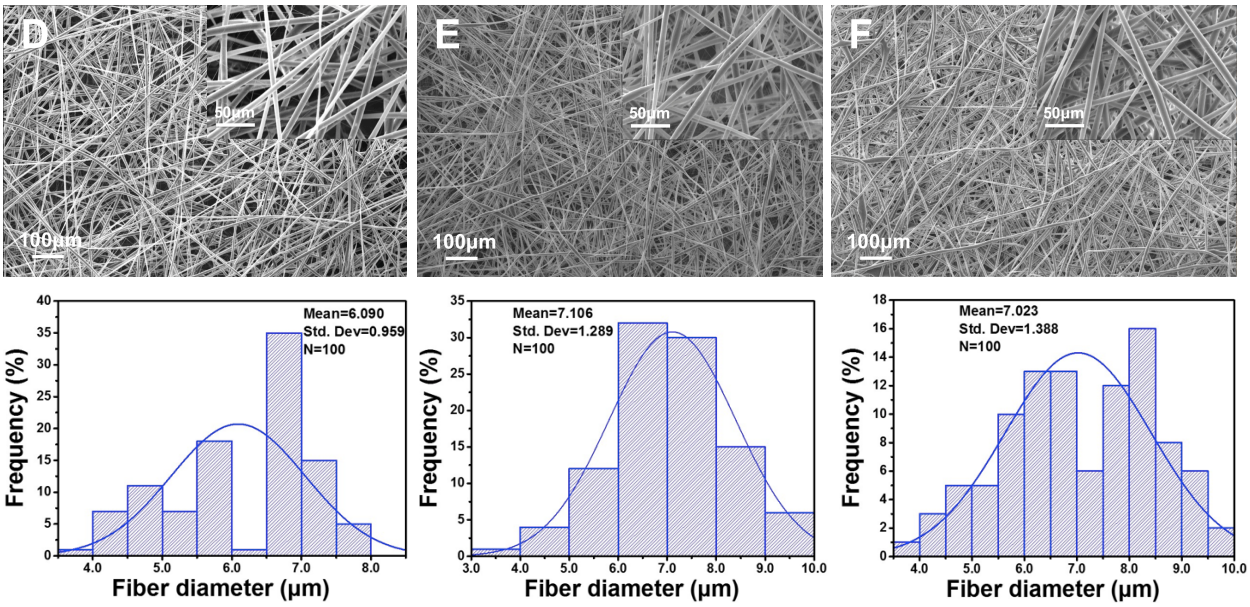

418

419

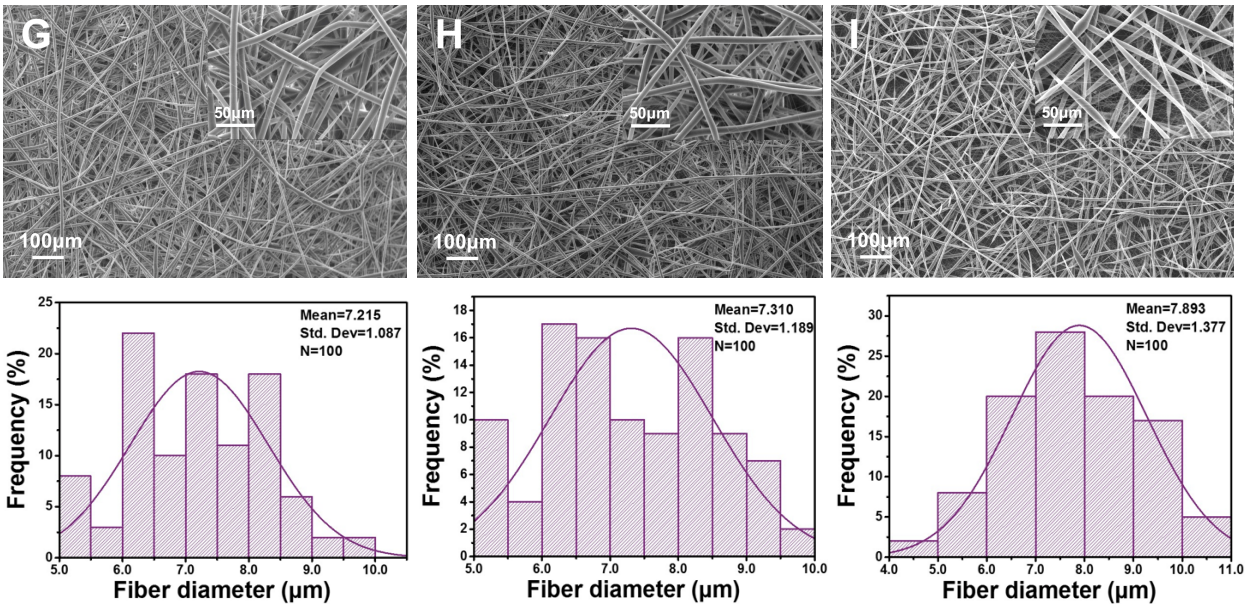

420

421

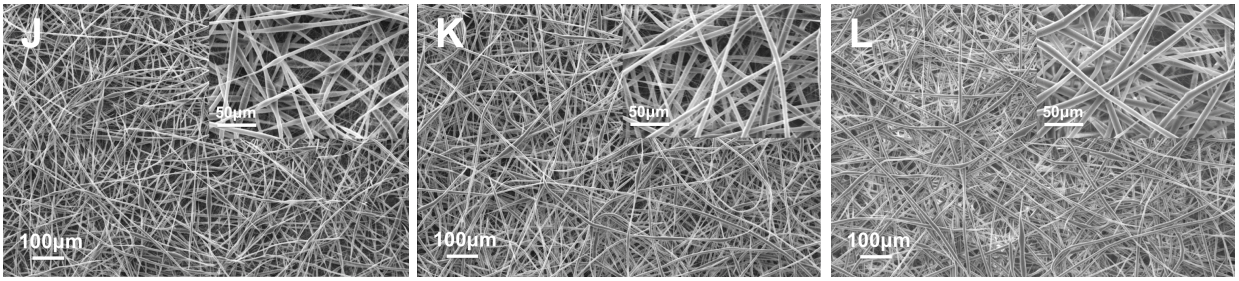

422

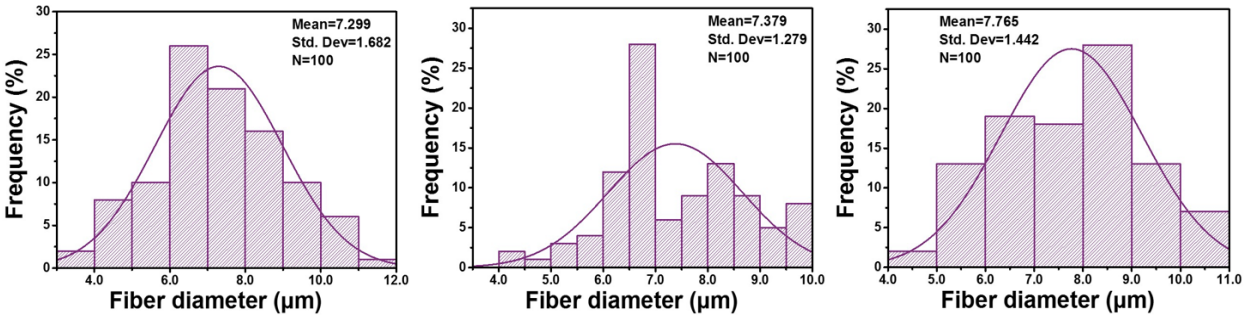

Figure 3. SEM images and fiber diameter distributions of pure (A-F) and P4-loaded (G-L) fibrous patches produced by ES. (A) 15cm, 10 μl/min, 6 kV (B) 15cm, 20 μl/min, 8 kV (C) 15cm, 30 μl/min, 10 kV (D) 13cm, 10 μl/min, 6 kV (E) 13cm, 20 μl/min, 8 kV (F) 13cm, 30 μl/min, 10 kV (G) 15cm, 10 μl/min, 12 kV (H) 15cm, 20 μl/min, 12 kV (I) 15cm, 30 μl/min, 12 kV (J) 13cm, 10 μl/min, 10 kV (K) 13cm, 20 μl/min, 10 kV (L) 13cm, 30 μl/min, 10 kV. The values represent working distance, flow rate and applied voltage, respectively. In all diameter distributions, n = 100.

3.2. Attenuated Total Reflection-Fourier Transform Infrared Spectroscopy (ATR-FTIR)

The molecular structures of P4 and PLA only and P4-loaded PLA fibrous patches produced by PG and ES are indicated in Figure 4A. For pure PLA, the characteristic absorption bands observed were: CH_3 and C-H stretching vibrations at 2994 and 2947 cm^{-1}, C=O stretching bands at 1750 cm^{-1}, CH_3 asymmetric scissoring at 1458 cm^{-1}, CH_3 and C-H bending vibrations at 1386 and 1358 cm^{-1}, C-O-C stretching vibration at 1265 cm^{-1}, ester C-O asymmetric stretching at 1182 cm^{-1}, ester C-O symmetric stretching at 1133 cm^{-1}, alcohol C-O stretching vibration at 1084 cm^{-1}, C-CH_3 stretching at 1042 cm^{-1}, O-H bending at 950 cm^{-1} and C-COO stretching at 873 cm^{-1} (Yu et al., 2014).

For pure P4, the characteristic peaks were: C=O stretching bands at C_3 and C_{20}

442 (two ketone groups at C_3 and C_{20}) at 1661 cm^{-1} and 1698 cm^{-1}, these typically separate
443 P4 from other steroids. Other peaks present were C-H asymmetrical stretching at 2923
444 cm^{-1}, C-H symmetric stretching at 2851 cm^{-1} and C=C-H bending at 870 cm^{-1} (Leimann
445 et al., 2015). Thus, weaker peaks for C=O stretching were observed between 1600 and
446 1700 cm^{-1} in both P4-loaded PLA fibrous patches, these prove the presence of P4.

447 **3.3. X-ray Powder Diffraction**

448 XRD studies were applied to P4 powders, pure PLA (12%) and P4-loaded PLA
449 fibrous patches to confirm the encapsulated P4 in the PLA fibrous patches. In the XRD
450 patterns of PLA and P4, several diffraction peaks were observed. The crystallinity of P4
451 was determined at 12.7 and 16.9 2Θ degrees, while the crystallinity for PLA was
452 detected at 21.2 and 22.1 2Θ degrees (Oliveira et al., 2013). In P4-loaded PLA fibrous
453 patches, it is confirmed that P4 was encapsulated in the PLA fibrous patches in its
454 crystalline form (Figure 4B). As a result, PLA rich domains were observed in both ATR-
455 FTIR and XRD spectra and characteristic peaks of PLA and P4 were also seen
456 (indicated with arrows).

457 **3.4. Differential Scanning Calorimetry (DSC)**

458 DSC analyses of the samples were performed to determine the effect of P4 and the
459 production technique on the morphological structure of PLA based fibrous patches. In
460 Figure 4C, the DSC curves of the PLA fibrous patches, produced by PG and ES
461 techniques, are given together with and without P4 in the temperature range of 0-240^{o}C.
462 The curves a and c in Figure 4C represent pure PLA samples, produced by ES and PG,
463 respectively. Whilst the glass transition temperature (Tg) and melting temperature (Tm)
464 of native PLA is 63^{o}C and 165^{o}C, respectively, these temperatures did not change

significantly with the pure PLA sample, produced by PG. However, the electrospun sample resulted in lower Tg and Tm temperatures, compared to native PLA (Tg=59^{o}C and Tm=164^{o}C). This could be due to the slightly lower crystallinity of the sample, caused by ES. Furthermore, to determine the molecular interactions between P4 and PLA at a molecular scale, we recorded the DSC curves of the sample, for both techniques. As observed from the curves b and d in Figure 4C, P4 caused lower Tm values than those of pure PLA samples produced by both techniques. This was due to the suppression of PLA crystallinity with P4 through intermolecular interactions (Demirkaya et al., 2015).

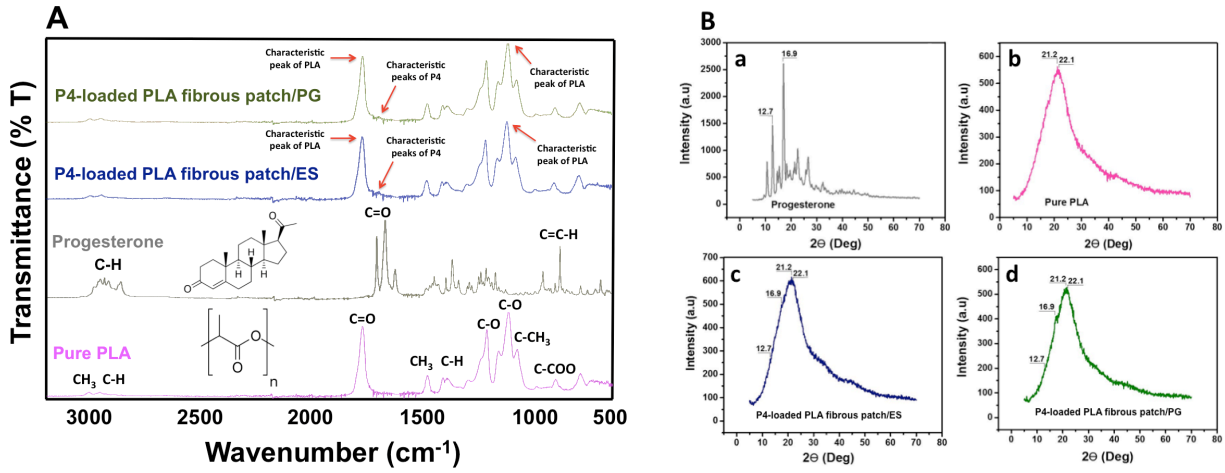

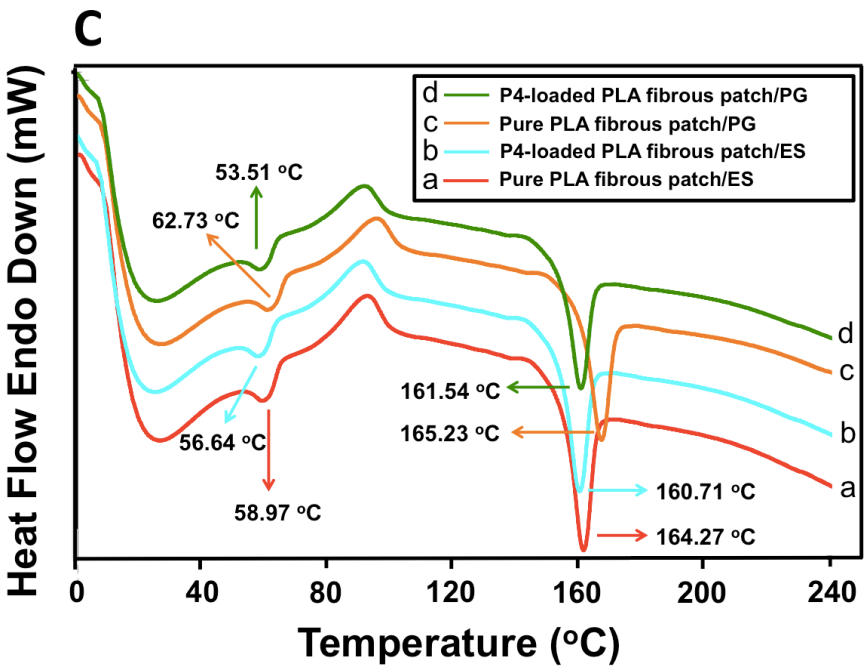
C
Heat Flow Endo Down (mW)
Temperature (°C)
d P4-loaded PLA fibrous patch/PG
c Pure PLA fibrous patch/PG
b P4-loaded PLA fibrous patch/ES
a Pure PLA fibrous patch/ES
53.51 °C
62.73 °C
56.64 °C
58.97 °C
161.54 °C
165.23 °C
160.71 °C
164.27 °C
0
40
80
120
160
200
240

475

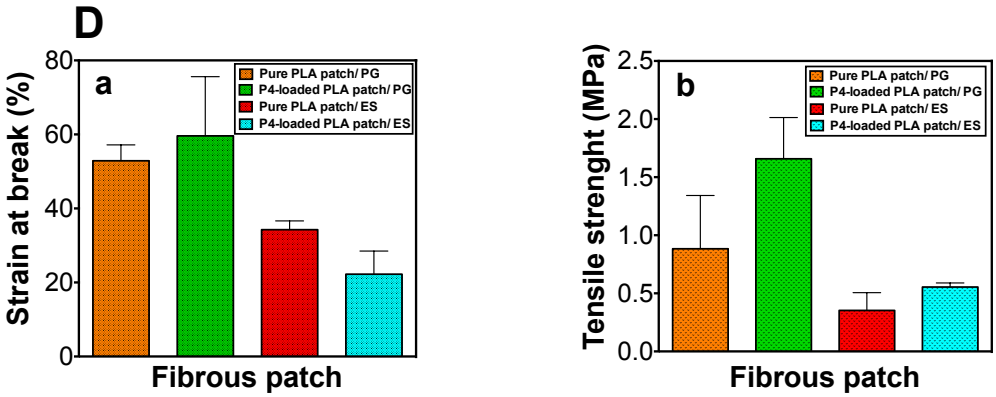
D
a
Strain at break (%)
Pure PLA patch/ PG
P4-loaded PLA patch/ PG
Pure PLA patch/ ES
P4-loaded PLA patch/ ES
Fibrous patch
b
Tensile strenght (MPa)
Fibrous patch

476

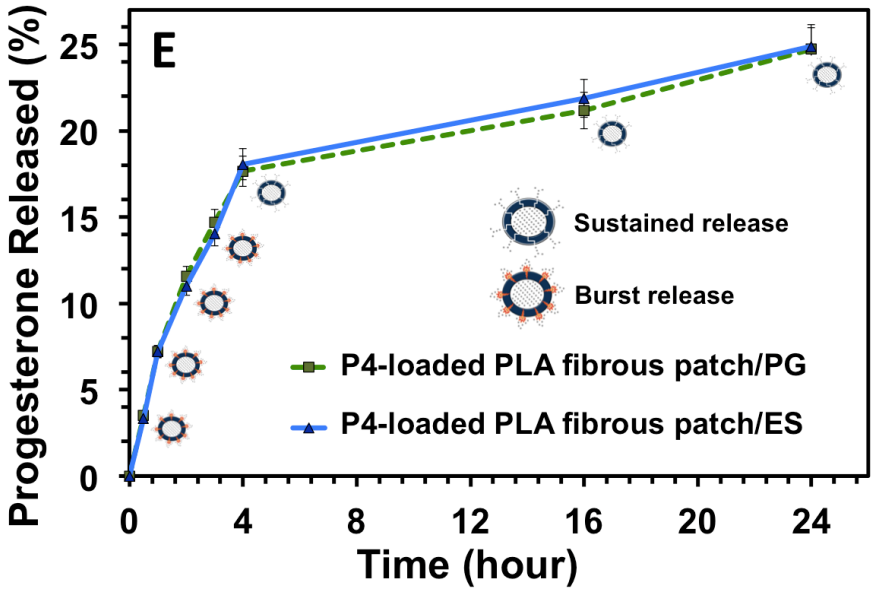
E
Progesterone Released (%)
Time (hour)
Sustained release
Burst release
P4-loaded PLA fibrous patch/PG
P4-loaded PLA fibrous patch/ES

477

Figure 4. Characterization of fibrous patches. (A) FTIR spectra of pure PLA, progesterone and P4-loaded PLA fibrous patches produced by PG and ES. (B) XRD patterns of (a) progesterone, (b) pure PLA, (c) P4-loaded PLA fibrous patches produced by ES and (d) PG. (C) DSC curves of pure and P4-loaded PLA fibrous patches produced by ES and PG. (D) Tensile properties of fibrous patches: (a) tensile strength and (b) strain at break. (E) Progesterone release profiles of P4-loaded fibrous patches, produced by PG and ES, according to first-order model. All the values were obtained from the averages of three experiments, and the errors were less than 5%.

3.5. Tensile Test of Fibrous Patches

Tensile strength and strain at break were investigated for each of the samples (Figure 4D). The loading of P4 into PLA increased the mechanical properties of the patches. As the P4 concentration increased in the PG technique, tensile strength of fibrous patches was enhanced, from 0.884 MPa to 1.658 MPa. This increase is also observed in ES with the addition P4 as seen by the increase in tensile strength from 0.353 MPa to 0.554 MPa. It is clearly seen that fibrous patches obtained by PG are more durable than with ES. We observed similar trends from the results of strain at break. As a result, it has been shown that the tensile strength increases as the diameter increases.

3.6. In Vitro Drug Release Studies

Initially, UV spectra was used to acquire the concentration range of P4 from 0,625 to 10 µg/mL and a linear standard calibration curve was created from P4 absorption values (R^2=0.9880). This spectrum was used for quantitative determination of the drug release. Although the fibrous patches were submerged in the simulated vaginal fluid, P4

passed through the membrane to PBS. The releasing profiles of P4-loaded fibrous patches were measured in PBS of pH 7.4 and a controlled temperature of 37^{o}C to mimic the normal physiological *in vivo* conditions. As shown in Figure 4E, P4 can be successfully released from fibrous patches over a period of 24 hours according to the first-order kinetic model; both production techniques exhibited sustained release in 24 hours (PG: 24.72% and ES: 24.89%). However, burst release was seen within first 4h in both fibrous patches (PG: 17.67% and ES: 18.06%). The drug encapsulation efficiency was calculated to be ~ 97% for both forming scenarios, PG and ES. As a result, P4 was released from both fibrous patches successfully and in a controlled manner. There is no significant difference between the forming techniques in terms of drug release.

3.7. In Vitro Cytotoxicity Studies

3.7.1. Cell Attachment

The initial cell attachment performance of the samples extracted from the developed fibrous patches as well as blank TCPS control is given as a percentage of the cell concentration initially seeded, in Figure 5A. Over the course of 3 h, the Vero cells were found to be attached to the surfaces of the samples as well as the blank TCPS controls with a steadily increasing tendency. Within the first hour of the initial seeding, the attachment on all fibrous patch samples reached almost 50% of the initial cell concentration where blank control managed to support only 25% of the cells initially seeded. At the end of the 3rd hour, the samples reached attachment concentration around ~75-80% and ~80-85% of the cells initially seeded for pure and P4-loaded patches, respectively. However, considering the statistical deviation of the results, the small amount of the initial cell concentration and the short duration of the assay, the

difference between pure and P4-loaded patches could be considered relatively small, and the difference between the patches produced with PG and ES was almost insignificant (~2-3%) to consider.

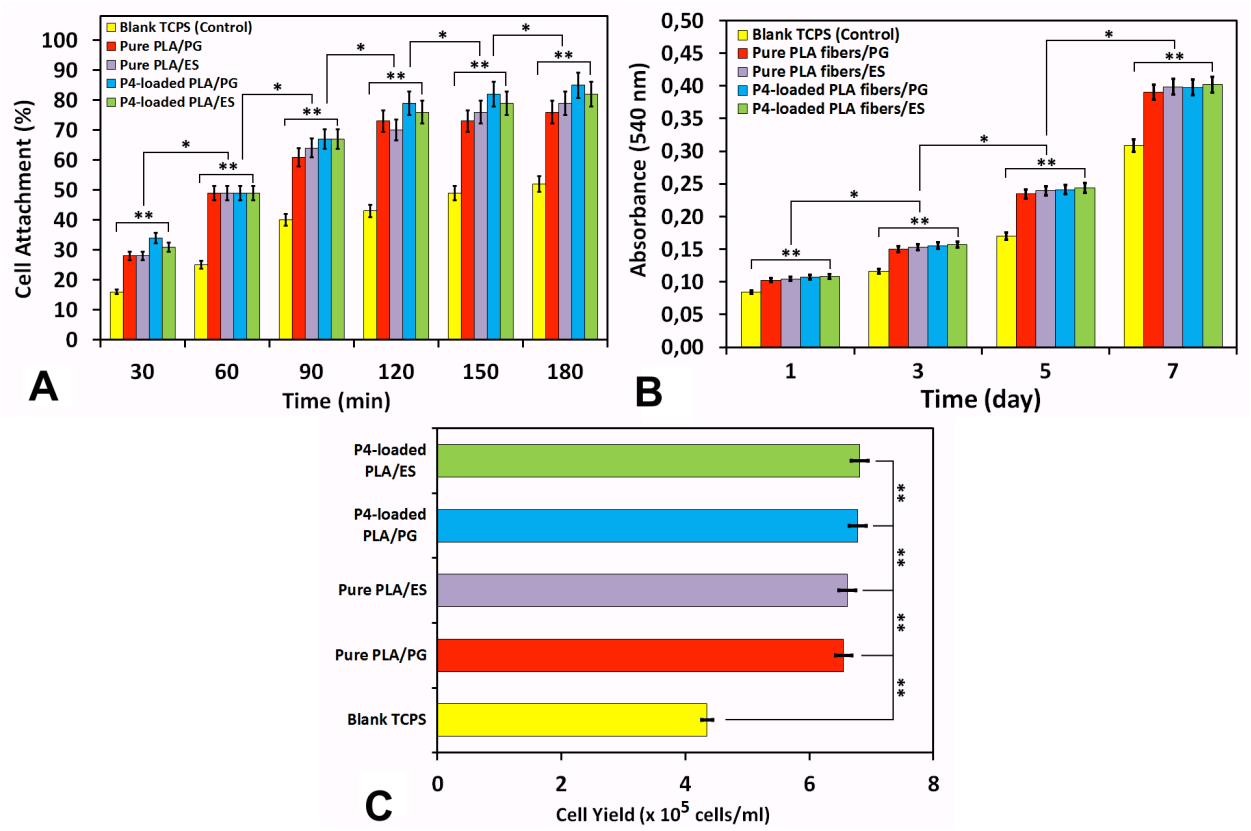

Figure 5. Cell culture results for fibrous patches. (A) 3 h attachment, (B) 7 day viability, and (C) cell yield (at 7th day) performances of the pure and progesterone-loaded fibrous

patches produced by PG and ES as well as blank TCPS control Petri dishes. The symbols "*" and "**" indicate the significant differences (* for $p < 0.05$ and ** for $p < 0.01$). (D) Fluorescence images obtained at the end of the 3rd day of culture: (A) pure PLA/PG, (B) pure PLA/ES, (C) P4-loaded PLA/PG, (D) P4-loaded PLA/ES fibrous patches, and at the end of the 7th day of culture from (E) pure PLA/PG, (F) pure PLA/ES, (G) P4-loaded PLA/PG, (H) P4-loaded PLA/ES fibrous patches. Magnifications: x40. Green: AF-488 stained actin filaments, Blue: DAPI stained nucleus. The statistical analyses were carried out with ANOVA tests with the Tukey multiple comparison test.

3.7.2. Viability and Yield

MTT assay is a colorimetric assay in which the determined values represent the cell viability and/or proliferation. The assay is based on the reduction of yellow colored tetrazolium dye to purple colored formazan crystals. The assay represents the cell viability and proliferation since this reduction is carried out by mitochondria of viable cells and the amount of reduction, which is measured in terms of absorption intensity, depends on the metabolic activity of the cells (Chen et al., 2014). Therefore, in this study, MTT assay was used as a measure of cell viability and/or proliferation. The absorbance intensity of the fibrous patches was initially found to be similar to the blank control dishes (Figure 5B). However, according to the measurements done over a total course of 7 days, as the culture progressed, the fibrous patches began to show higher absorbance than TCPS controls as a result of increased metabolic activity due to their high surface area provided by their fibrous structures, similar in observation during the initial attachment performances. As a result, the metabolic activity continued to increase

554 steadily at 48 h intervals without showing any cytotoxicity for the Vero cells. The blank
555 controls were also performed sufficiently in the culture without any cytotoxicity as
556 expected from commercial TCPS dishes (Maghdouri-White et al., 2014). The cell yields
557 obtained at the end of the culture showed consistent results with 7-day MTT assay as it
558 showed that the fibrous structure of the patches provided additional anchorage points
559 for cells to attach and proliferate, not only on the surface but also within the patch since
560 the number of cells counted on the patches exceeded the number of cells that can
561 possibly proliferate as a monolayer on a 1 cm^2 surface (Figure 5C). Since, the
562 increased cell yield as well as the constant increase in the metabolic activity according
563 to the MTT assay can be interpreted as the increase in the cell number, the cell
564 functionality as well as the cell viability (Pagliacci et al., 1993), it can be concluded that
565 the fibrous patches provided a more suitable environment for cells to stay healthy and
566 viable throughout the course of 7 days.

567 **3.7.3. Visual Inspection**

568 In addition to quantitative assays, the culture was also monitored visually to inspect
569 any changes in morphology of the cells seeded on the produced fibrous patches. For
570 sufficient coverage of the culture progress, the mid-period and end-period were
571 inspected. Therefore, images of the cultured samples were obtained at the end of the
572 3^{rd} and the 7^{th} day of the culture from AF-488/DAPI dual stained samples by using
573 fluorescence microscopy. AF-488 and DAPI are both widely used fluorescence stains to
574 label actin filaments of cytoskeleton and nucleus of the cells, respectively. The dual
575 utilization of these stains can provide good visualization of the cell morphology. The
576 fluorescence images obtained from the cultured samples were consistent with the

previous quantitative assay results (Figure 5D). Even on the 3rd day of the culture, the cell population density on all samples was significantly high and the well-defined Vero cell morphology was intact. At the end of the culture, it can be seen that not only the surface of the samples was highly covered with almost a monolayer of cells, but also cells have grown on top of each other in a 3 dimensional pattern (out of focus and less bright cells).

3.8. In Vitro Organ Bath Experiments

The results obtained from the in vitro organ bath are given below as responses to KCl and cumulative (-)-noradrenaline. In vivo tests were completed with only P4-loaded fibrous patches/ES because the fibrous patches obtained by ES had several advantages compared to PG technique such as better morphology, smaller fiber diameter and also ES is a commonly used technique.

3.8.1. Contracting Effect of KCl

Results of isolated organ bath experiment studied on the 22-day-pregnant rats demonstrated that P4-loaded fibrous patches/ES decreased myometrial contracting effect at 124 mM KCl ($p<0.05$), which may be acted via voltage-gated calcium channels (Figure 6A). These changes in the KCl response may be due to changes in calcium influx (Grazzini et al., 1998).

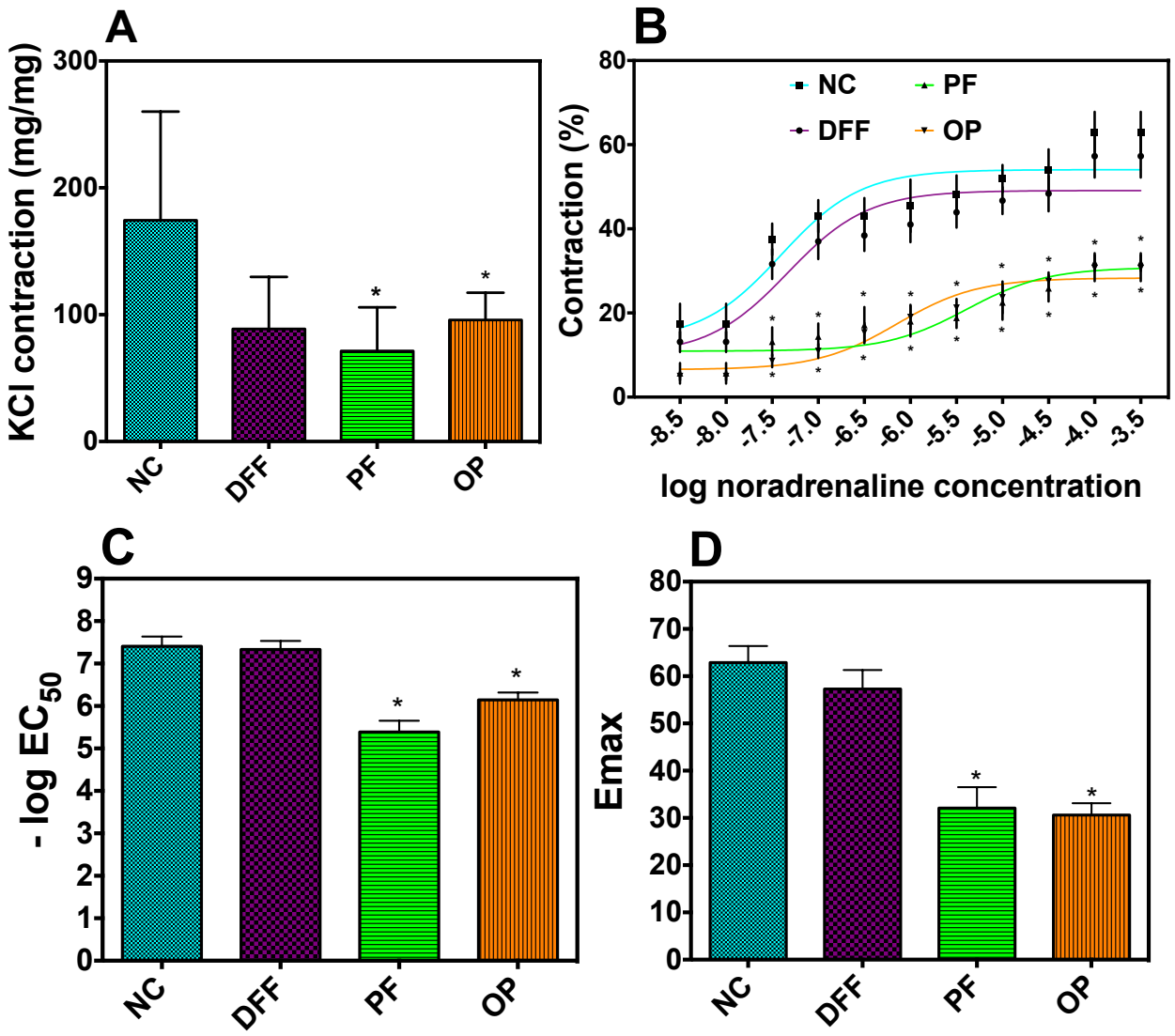

Figure 6. In vitro organ bath experiment's results. (A) In vitro organ bath contraction of rat uterine smooth muscle induced by 124 mM KCl in the 22-day-pregnant rat myometrium with progesterone treatments. *p<0.05 versus naive control group. (B) Effects of progesterone treatments on the (-)-noradrenaline-evoked contractions in the 22-day-pregnant rat myometrium. *p<0.05 versus naive control group and drug-free fibrous patch implantation group. Changes in contraction intensity were calculated using the areas under the curve and expressed as mean ± SEM (n=6). (C and D) Changes in the uterus contracting effect of (-)-noradrenaline (EC_{50} and Emax values, respectively)

in the 22-day-pregnant rat myometrium with progesterone treatment. *p<0.05 versus naive control group and drug-free fibrous patch implantation group. The statistical analyses were carried out with ANOVA tests with the Tukey multiple comparison test. NC: Naive control group, DFF: Drug-free fibrous patch implantation group, PF: Progesterone-loaded fibrous patch/Electrospinning implantation group, OP: Oral progesterone group, EC_{50}: The contractions of (-)-noradrenaline, which elicits half of the maximum contracting effect of (-)-noradrenaline, Emax: The maximum contracting effect of (-)-noradrenaline.

3.8.2. Contracting Effect of Cumulative (-)-Noradrenaline

Myometrial contracting effect of (-)-noradrenaline in the concentration range of $10^{-8.5}$-$10^{-3.5}$ M in the 22-day-pregnant myometrium is shown in Figure 6B. In the previous studies, P4 showed a relaxing effect on the contractions (Kubli-Garfias et al., 1983). Similar results have been reported on muscle rings from pregnant and non-pregnant human uterus in vitro (Beck et al., 1982).

P4-loaded fibrous patch/ES and oral P4 treatments decreased the myometrial contracting effect of (-)-noradrenaline in the concentration range of $10^{-7.5}$-$10^{-3.5}$ M when compared with the naive control group and the drug-free fibrous patch implantation group ($p<0.05$). But these treatments did not decrease the myometrial contracting effect of (-)-noradrenaline in the concentration range of $10^{-8.5}$-10^{-8} compared with the naive control group and the drug-free fibrous patches implantation groups. In addition, oral P4 treatment caused lower myometrial contractions (Emax=30.6 ± 2.5) compared with the P4-loaded fibrous patch/ES implantation group (Emax=32.1 ± 4.4), but there is no significant difference between these groups at any concentrations. According to these

results, the relaxing effect of P4 was moderated at low concentrations ($10^{-8.5}$-10^{-8}) of (-)-noradrenaline, while the relaxing effect is greater in concentrations over $10^{-7.5}$ in both the oral and fibrous patch treatment groups.

The curves of EC50 and Emax values are shown in Figure 6C and 6D, respectively. P4 treatments reduced the maximum myometrial contracting effect and the EC_{50} values of (-)-noradrenaline.

4. Discussion

P4-loaded fibrous patches were created for the intra-vaginal application using two different techniques, ES and PG, to prevent preterm birth. The characterization of solutions and patches, in vitro and in vivo analyses of patches were provided and also production techniques were compared.

As it is well known, fiber size and morphology are affected by solution viscosity in both methods (Ahmed et al., 2018). Bead and droplet defects are observed in SEM when the polymer concentration is low. In this case, electrospraying occurs instead of ES where beads are formed instead of fibers. There is a direct correlation between viscosity and fiber morphology, at higher viscosities the fibers have larger diameters. The surface tension of the polymer solutions has a crucial role in influencing the ES and PG fiber formation. As the surface tension needs to be overcome in order to form fibers with both techniques, a high surface tension can cause fibers to not form or be heavily beaded (Brako et al., 2018). In ES, the augmentation in electrical conductivity leads to the formation of smaller, bead-free fibers.

After production of patches by both techniques, morphological characterizations were done and the increase of polymer concentration caused the rise in the diameter of the fibers and also, adding P4 to the solutions made the fibers thicker. The addition of P4 to lower than 12% PLA solution caused heavily beaded fibers and loss in homogeneity. Fibers with 12% PLA + P4 solution were homogeneously dispersed and distributed within the polymer matrices, and the highest production yield per ml solution also belonged to the 12% PLA. Therefore, it can said that PG has an advantage compared to ES in production yield.

ATR-FTIR and XRD were used to confirm that the drug was successfully encapsulated. The FTIR results identified that there was no serious polymer-drug interaction. The halo diffraction pattern sighted between 10 and 40 2Θ is the characteristic of amorphous material verifying a degree of amorphous characteristics in the drug-loaded fibrous patches. It is most probably related to the polymeric carrier (Jain et al., 2008).

It is well known that, human body temperature varies between 36.1°C and 37.8°C in healthy individuals and fluctuates by about 0.5°C during the day. Internal vaginal temperature is ~ 37^{o}C (Boyd et al., 2015). A body temperature rises over 40°C is considered very-high, and temperatures over 41.5^{o}C cause hyperthermia. According to the DSC results, P4-loaded PLA fibrous patches can safely be applied by the intra-vaginal route without risk of melting and also P4 and PLA exhibited intermolecular interactions and, thus, distributed the PLA crystallinity (Demirkaya et al., 2015).

Drug release studies of P4-loaded fibrous patches were performed according to the first-order kinetic model. Here a Franz diffusion cell with cellulose acetate membrane

673 and simulated vaginal fluid was used to investigate P4 release from fibrous patches
674 across an artificial membrane mimicking the mucosal environment of the vagina. These
675 tests indicated whether or not the required amount of drug was released from fibrous
676 patches in the clinically feasible period. These results were also used in the planning of
677 in vivo tests. As a result, P4 was released from both fibrous patches successfully and in
678 a controlled manner. Therefore, the same effect on maintenance tocolysis can be
679 obtained with reduced frequency of dosage and the amount of drug.

680 The cytotoxicity of the pure and P4-loaded fibrous patches produced by PG and ES
681 were conducted with Vero epithelial cells, and TCPS Petri dishes, which are
682 commercially used for routine cell culture, and used as the blank to compare the
683 performance. The result obtained from cell culture test was a clear outcome of the
684 fibrous/porous 3 dimensional structures of the samples, which provided a distinctive
685 advantage in terms of attachment compared to the 2 dimensional surfaces of the blank
686 TCPS. Since the Vero cells, as with all animal cells, are anchorage-dependent, these
687 fibrous/porous 3 dimensional structures became a better host for them because of the
688 higher amount of focal points for cells to adhere due to their surface area (Ozkan and
689 Turkoglu Sasmazel, 2016). Besides, the most important outcome of the assay
690 conducted was that the patches prepared with either method, whether they were drug
691 loaded or not, did not affect the cell attachment mechanism negatively, which indicated
692 no short term cytotoxicity and considerably more attachment compared to blank controls
693 because of the fibrous structure. The fibrous patches showed better cell proliferation
694 because of the advantage gained during the initial cell attachment, resulting in early
695 initiation of the metabolic activity and better overall proliferation of the cells at the end of

7 days (Maghdouri-White et al., 2014). Both the pure and P4-loaded fibrous patches, whether produced with PS or ES, performed similarly compared to each other without showing any significant difference in performance; therefore, it should be noted that neither PLA nor P4-loading or the production methods caused any kind of cytotoxicity or negative effect on viability and proliferation of the Vero cells. Because of the non-woven fibrous structure, the cells attached faster and in larger quantities which resulted this better 7-day performance of the patches (Ozkan and Turkoglu Sasmazel, 2017). It can also be noted that there is not enough observable significant differences between PG or ES produced patches or pure or P4-loaded patches. As a result, it can be concluded by the ability to grow in larger quantities without any observable morphology changes, clearly shows that, similar to the previous quantitative analyses, fibrous patches developed with both methods, whether loaded with P4 or not, do not have any cytotoxicity on the morphology or growth of the Vero cells. It can be said that there is no significant difference according to the results of drug release tests, DSC tests and cell culture tests between production techniques. Therefore, PG can be used for scale-up of production with many advantages such as better production yield and tensile strength.

P4 plays a major role in the myometrial function during gestation, the main focus of our study was to clarify the effects of P4-loaded PLA fibrous patches in late-pregnant uterine functions and compare these with oral P4 treatments on rats in organ bath experiments. The mechanism of the effect of maintenance tocolysis with P4 has been demonstrated in previous studies. P4 increases the synthesis of B_2-adrenoceptors during pregnancy and participates in the regulation of G-proteins in the myometrium (Riemer et al., 1988; Rossier et al., 1999). P4-loaded fibrous patches were inserted into

719 vagina of pregnant rats on the 15th day of the pregnancy. Oral P4 treatment began on
720 the 15th day of the pregnancy and continued to the 21st day, this treatment period was
721 equivalent to the third trimester of human pregnancy. On the 22nd day of pregnancy, all
722 the rats were decapitated and the uterine tissues were removed. The frequency of the
723 dosage and its side effects will be reduced with patches compared to daily oral P4
724 treatment. The results obtained from the in vitro organ bath experiment showed that
725 both P4-loaded fibrous patch and oral P4 treatment decrease myometrial contraction of
726 both KCl and cumulative (-)-noradrenaline on pregnant rat uterus. The P4-loaded
727 fibrous patch/ES implantation group inhibited uterine contractions as well as the oral P4
728 group and there is no significant difference between them. Consequently, P4 can be
729 loaded into PLA fibers, thereby offering high bioavailability, fewer systemic side effects,
730 and reduced frequency of dosage by the controlled release feature.

731

732 ## 5. Conclusion

733 In summary, we have engineered intra-vaginal P4-loaded PLA fibrous patches and
734 these patches can be used in the treatment of preterm birth with some advantages. Two
735 different techniques, ES and PG, were performed to produce fibrous patches and both
736 were extensively compared. When the diameter of P4-loaded fibrous patches were
737 compared, fibrous patches containing fibers with a smaller diameter was obtained by
738 ES compared to PG. PG had two advantages compared to ES; better production rate
739 and higher tensile strength. Our results indicated that both techniques showed
740 sustained P4 release with a similar profile. DSC results of fibrous patches were similar
741 and they can be safely applied via the intra-vaginal route without degradation. The

patches did not affect the cell attachment, viability and proliferation on Vero cells negatively. PG patches were produced at a much faster rate making them suitable for more high demand application as seen for this type of medication. Following release studies and cell culture tests, in vivo tests were conducted in order to investigate the effect of maintenance tocolysis with P4-loaded fibrous patches. Fibrous patches significantly decreased uterine contractions as much as the standard oral route. Consequently, both techniques (PG and ES) are successful in the production of P4-loaded fibrous polymeric patches, which are a novel and beneficial treatment strategy with high bioavailability, reduced frequency of dosage, and the amount of drug.

Acknowledgments

The authors are grateful to the UK Engineering & Physical Sciences Research Council (EPSRC) for funding pressurized gyration forming research at University College London (Grants EP/S016872/1 and EP/N034228/1). Dr. M.E. Cam was supported by a TUBITAK 2219 Research Programme Grant (Scientific and Technological Research Council of Turkey-TUBITAK) and thanks UCL Mechanical Engineering for hosting his post-doctoral research in the UK.

Declaration of interest

The authors declare no conflict of interest.

Appendix A. Supplementary data

Supplementary data associated with this article can be found, in the online version.

References

Ahmed, J., Matharu, R.K., Shams, T., Illangakoon, U.E., Edirisinghe, M., 2018. A Comparison of Electric-Field-Driven and Pressure-Driven Fiber Generation Methods for Drug Delivery. Macromol. Mater. Eng. 303, 1700577.

Alenezi, H., Cam, M.E., Edirisinghe, M., 2019. Experimental and theoretical investigation of the fluid behavior during polymeric fiber formation with and without pressure. Appl. Phys. Rev. 6, 041401.

Balamurugan, R., Sundarrajan, S., Ramakrishna, S., 2011. Recent Trends in Nanofibrous Membranes and Their Suitability for Air and Water Filtrations. Membranes 1, 232-248.

Beck, P., Adler, P., Szlachter, N., Goldsmith, L.T., Steinetz, B.G., Weiss, G., 1982. Synergistic effect of human relaxin and progesterone on human myometrial contractions. Int. J. Gynaecol. Obstet. 20, 141-144.

Boyd, P., Desjardins, D., Kumar, S., Fetherston, S.M., Le-Grand, R., Dereuddre-Bosquet, N., Helgadóttir, B., Bjarnason, Á., Narasimhan, M., Malcolm, R.K., 2015. A temperature-monitoring vaginal ring for measuring adherence. PloS one 10, e0125682-e0125682.

Brako, F., Raimi-Abraham, B.T., Mahalingam, S., Craig, D.Q.M., Edirisinghe, M., 2018. The development of progesterone-loaded nanofibers using pressurized gyration: A novel approach to vaginal delivery for the prevention of pre-term birth. Int. J. Pharm. 540, 31-39.

784 Cam, M.E., Cesur, S., Taskin, T., Erdemir, G., Kuruca, D.S., Sahin, Y.M., Kabasakal, L.,
785 Gunduz, O., 2019a. Fabrication, characterization and fibroblast proliferative activity of
786 electrospun Achillea lycaonica-loaded nanofibrous mats. Eur. Poly. J. 120, 109239.
787 Cam, M.E., Yildiz, S., Alenezi, H., Cesur, S., Ozcan, G.S., Erdemir, G., Edirisinghe, U.,
788 Akakin, D., Kuruca, D.S., Kabasakal, L., Gunduz, O., Edirisinghe, M., 2020. Evaluation
789 of burst release and sustained release of pioglitazone-loaded fibrous mats on diabetic
790 wound healing: an in vitro and in vivo comparison study. J. R. Soc. Interface 17,
791 20190712.
792 Cam, M.E., Zhang, Y., Edirisinghe, M., 2019b. Electrosprayed microparticles: a novel
793 drug delivery method. Expert Opin. Drug Del. 16, 895-901.
794 Chen, S.-H., Chang, Y., Lee, K.-R., Lai, J.-Y., 2014. A three-dimensional dual-layer
795 nano/microfibrous structure of electrospun chitosan/poly(d,l-lactide) membrane for the
796 improvement of cytocompatibility. J. Membrane Sci. 450, 224-234.
797 Demirkaya, Z.D., Sengul, B., Eroglu, M.S., Dilsiz, N., 2015. Comprehensive
798 characterization of polylactide-layered double hydroxides nanocomposites as packaging
799 materials. J. Polym. Res. 22, 1-13.
800 Goldenberg, R.L., Culhane, J.F., Iams, J.D., Romero, R., 2008. Epidemiology and
801 causes of preterm birth. Lancet 371, 75-84.
802 Goletiani, N.V., Keith, D.R., Gorsky, S.J., 2007. Progesterone: Review of safety for
803 clinical studies. Exp. Clin. Psychopharm. 15, 427-444.
804 Graham, J.D., Clarke, C.L., 1997. Physiological action of progesterone in target tissues.
805 Endocr. Rev. 18, 502-519.

Grazzini, E., Guillon, G., Mouillac, B., Zingg, H.H., 1998. Inhibition of oxytocin receptor function by direct binding of progesterone. Nature 392, 509.

Hajagos-Tóth, J., Bóta, J., Ducza, E., Samavati, R., Borsodi, A., Benyhe, S., Gáspár, R., 2016. The effects of progesterone on the alpha2-adrenergic receptor subtypes in late-pregnant uterine contractions in vitro. Repod. Biol. Endocrinol. 14, 33-33.

Heseltine, P.L., Ahmed, J., Edirisinghe, M., 2018. Developments in Pressurized Gyration for the Mass Production of Polymeric Fibers. Macromol. Mater. Eng. 303, 1800218.

Huang, C.-K., Zhang, K., Gong, Q., Yu, D.-G., Wang, J., Tan, X., Quan, H., 2020. Ethylcellulose-based drug nano depots fabricated using a modified triaxial electrospinning. Int. J. Biol. Macromol. 152, 68-76.

Jain, S.K., Jain, A., Gupta, Y., Kharya, A., 2008. Design and development of a mucoadhesive buccal film bearing progesterone. Pharmazie 63, 129-135.

Karuppannan, C., Sivaraj, M., Kumar, J.G., Seerangan, R., Balasubramanian, S., Gopal, D.R., 2017. Fabrication of Progesterone-Loaded Nanofibers for the Drug Delivery Applications in Bovine. Nanoscale Res. Lett. 12, 116-116.

Khan, I., Ahmed, N., 1969. Effects of progesterone therapy on the stilboestrol-induced sensitivity of isolated rat uterus preparations. Br. J. Pharmacol. 35, 332-338.

Khdair, A., Hamad, I., Al-Hussaini, M., Albayati, D., Alkhatib, H., Alkhalidi, B., 2013. In vitro artificial membrane-natural mucosa correlation of carvedilol buccal delivery. J. Drug Del. Sci. Tech. 23, 602-609.

Kim, I.D., Ahn, K.H., Lee, S., Hong, S.C., Kim, S.H., Kim, T., 2013. Effect of ovariectomy, 17-beta estradiol, and progesterone on histology and estrogen receptors

of bladder in female partial bladder outlet obstruction rat model. J. Obstet. Gynaecol. Res. 39, 1259-1267.

Kim, N.N., Min, K., Pessina, M.A., Munarriz, R., Goldstein, I., Traish, A.M., 2004. Effects of ovariectomy and steroid hormones on vaginal smooth muscle contractility. Int. J. Impot. Res. 16, 43-50.

Kindinger, L.M., Bennett, P.R., Lee, Y.S., Marchesi, J.R., Smith, A., Cacciatore, S., Holmes, E., Nicholson, J.K., Teoh, T.G., MacIntyre, D.A., 2017. The interaction between vaginal microbiota, cervical length, and vaginal progesterone treatment for preterm birth risk. Microbiome 5, 6.

Kubli-Garfias, C., Hoyo-Vadillo, C., Lopez-Nieto, E., Ponce-Monter, H., 1983. Inhibition of spontaneous contractions of the rat pregnant uterus by progesterone metabolites. Proc. West Pharmacol. Soc. 26, 115-118.

Leimann, F.V., Heloisa Biz, M., Kaufmann, K.C., Maia, W.J., Hess Honçalves, O., Cardozo Filho, L., Sayer, C., Hermes de Araújoli, P.H., 2015. Characterization of progesterone loaded biodegradable blend polymeric nanoparticles. Ciência Rural 45, 2082-2088.

Maghdouri-White, Y., Bowlin, G.L., Lemmon, C.A., Dréau, D., 2014. Mammary epithelial cell adhesion, viability, and infiltration on blended or coated silk fibroin-collagen type I electrospun scaffolds. Mat. Sci. Eng C-Mater. 43, 37-44.

Mahalingam, S., Edirisinghe, M., 2013. Forming of polymer nanofibers by a pressurised gyration process. Macromol. Rapid Commun. 34, 1134-1139.

McCormick, M.C., Litt, J.S., Smith, V.C., Zupancic, J.A., 2011. Prematurity: an overview and public health implications. Annu. Rev. Public Health 32, 367-379.

Mofidfar, M., Prausnitz, M.R., 2019. Electrospun Transdermal Patch for Contraceptive Hormone Delivery. Curr Drug Deliv. 16, 577-83.

Nold, C., Maubert, M., Anton, L., Yellon, S., Elovitz, M.A., 2013. Prevention of preterm birth by progestational agents: what are the molecular mechanisms? Am. J. Obstet. Gynecol. 208, 223.e221-227.

Oliveira, J.E., Medeiros, E.S., Cardozo, L., Voll, F., Madureira, E.H., Mattoso, L.H.C., Assis, O.B.G., 2013. Development of poly(lactic acid) nanostructured membranes for the controlled delivery of progesterone to livestock animals. Mater. Sci. Eng. C 33, 844-849.

Owen, D.H., Katz, D.F., 1999. A vaginal fluid simulant. Contraception 59, 91-95.

Ozkan, O., Turkoglu Sasmazel, H., 2016. Effects of nozzle type atmospheric dry air plasma on L929 fibroblast cells hybrid poly (ε-caprolactone)/chitosan/poly (ε-caprolactone) scaffolds interactions. J. Biosci. Bioeng. 122, 232-239.

Ozkan, O., Turkoglu Sasmazel, H., 2017. Hybrid polymeric scaffolds prepared by micro and macro approaches. Int. J. Polym. Mater. Po. 66, 853-860.

Pagliacci, M.C., Spinozzi, F., Migliorati, G., Fumi, G., Smacchia, M., Grignani, F., Riccardi, C., Nicoletti, I., 1993. Genistein inhibits tumour cell growth in vitro but enhances mitochondrial reduction of tetrazolium salts: a further pitfall in the use of the MTT assay for evaluating cell growth and survival. Eur. J. Cancer 29a, 1573-1577.

Qin, Z.-Y., Jia, X.-W., Liu, Q., Kong, B.-h., Wang, H., 2019. Fast dissolving oral films for drug delivery prepared from chitosan/pullulan electrospinning nanofibers. Int. J. Biol. Macromol. 137, 224-231.

Raimi-Abraham, B.T., Mahalingam, S., Davies, P.J., Edirisinghe, M., Craig, D.Q., 2015. Development and Characterization of Amorphous Nanofiber Drug Dispersions Prepared Using Pressurized Gyration. Mol. Pharm. 12, 3851-3861.

Riemer, R.K., Wu, Y.Y., Bottari, S.P., Jacobs, M.M., Goldfien, A., Roberts, J.M., 1988. Estrogen reduces beta-adrenoceptor-mediated cAMP production and the concentration of the guanyl nucleotide-regulatory protein, Gs, in rabbit myometrium. Mol. Pharmacol. 33, 389-395.

Rossier, O., Abuin, L., Fanelli, F., Leonardi, A., Cotecchia, S., 1999. Inverse agonism and neutral antagonism at alpha(1a)- and alpha(1b)-adrenergic receptor subtypes. Mol. Pharmacol. 56, 858-866.

Wilson, P., 2009. Development and validation of a liquid chromatographic method for the simultaneous determination of estradiol, estriol, estrone, and progesterone in pharmaceutical preparations. J AOAC Int. 92, 846-854.

Yu, T., Jiang, N., Li, Y., 2014. Study on short ramie fiber/poly(lactic acid) composites compatibilized by maleic anhydride. Compos. Part A-Appl. S. 64, 139-146.